can have an approximate value of Γ^* as high as approximately one-eighth that of the Kármán vortices. This ratio is likely higher for image 3, where the shear-layer vortices attain larger values of Γ^*.

Conclusions

Over a range of Reynolds number represented by $Re = 5 \times 10^3$, the Kármán vortices form relatively far downstream of the cylinder. Moreover, the small-scale, shear-layer vortices formed immediately downstream of separation exhibit different rates of development and symmetry from cycle to cycle of the Kármán vortex formation. In turn, the nature of the shear-layer vortex system is linked to the location and orientation of the eventually formed Kármán vortex. When the vortices develop symmetrically in the opposing shear layers, and quickly attain relatively large values of circulation, the Kármán vortex is formed further downstream.

The instantaneous circulation of the vortices can reach a value as large as one-eighth that of the Kármán vortex. Attempts to deduce this circulation, using phase-referenced measurements triggered on the Kármán vortex, are not meaningful because the shear-layer vortices are not phase locked to the Kármán vortices.

Further efforts should address the spanwise correlation of the shear-layer and Kármán vortex development to determine the degree to which the foregoing observations are influenced by three-dimensional distortions.

Acknowledgments

The authors gratefully acknowledge the financial support of the Office of Naval Research through Grants N00014-94-1-0185 and N00014-90-J-1510, monitored by Thomas Swean.

References

[1]Bloor, M. S., "The Transition to Turbulence in the Wake of a Circular Cylinder," *Journal of Fluid Mechanics*, Vol. 19, Pt. 2, 1964, pp. 290–319.

[2]Gerrard, J. H., "A Disturbance-Sensitive Reynolds Number Range of Flow Past a Circular Cylinder," *Journal of Fluid Mechanics*, Vol. 22, Pt. 1, 1965, pp. 187–196.

[3]Gerrard, J. H., "The Wakes of a Cylindrical Bluff Body at Low Reynolds Number," *Philosophical Transactions of the Royal Society of London, Series A: Mathematical and Physical Sciences*, Vol. 288, 1978, pp. 351–382.

[4]Wei, T., and Smith, C. R., "Secondary Vortices in the Wake of Circular Cylinders," *Journal of Fluid Mechanics*, Vol. 169, Aug. 1986, pp. 513–533.

[5]Kourta, A., Boisson, H. C., Chassing, P., and Haminh, H., "Nonlinear Interaction and the Transition to Turbulence in the Wake of a Circular Cylinder," *Journal of Fluid Mechanics*, Vol. 181, Aug. 1987, pp. 141–161.

[6]Unal, M. F., and Rockwell, D., "On Vortex Formation from a Cylinder. Part 1. The Initial Instability," *Journal of Fluid Mechanics*, Vol. 190, May 1988, pp. 491–512.

[7]Filler, J. R., Marston, P. L., and Mieh, W. C., "Response of the Shear Layer Separating from a Circular Cylinder to Small-Amplitude Rotational Oscillations," *Journal of Fluid Mechanics*, Vol. 231, Oct. 1991, pp. 481–499.

[8]Ahmed, A., Khan, M. J., and Bays-Muchmore, B., "Experimental Investigation of a Three-Dimensional Bluff-Body Wake," *AIAA Journal*, Vol. 31, No. 3, 1993, pp. 559–563.

[9]Sheridan, J., Soria, J., Wu, J., and Welsh, M. C., "The Kelvin–Helmholtz Instability of the Separated Shear Layer from a Circular Cylinder," *Bluff-Body Wakes, Dynamics and Instabilities*, edited by H. Eckelmann, J. M. Graham, P. Huerre, and P. A. Monkewitz, Proceedings of IUTAM Symposium (Goettingen, Germany, Sept. 1992), Springer–Verlag, Berlin, 1993, pp. 115–117.

[10]Chyu, C.-K., Lin, J.-C., Sheridan, J., and Rockwell, D., "Kármán Vortex Formation from a Cylinder: Role of Phase-Locked Kelvin–Helmholtz Vortices," *Physics of Fluids*, Vol. 7, No. 9, 1995, pp. 2288–2290.

[11]Lin, J.-C., Towfighi, J., and Rockwell, D., "Instantaneous Structure of Near-Wake of a Circular Cylinder: On the Effect of Reynolds Number," *Journal of Fluids and Structures*, Vol. 9, 1995, pp. 659–669.

[12]Chyu, C.-K., "A Study of the Near-Wake Structure from a Circular Cylinder," Ph.D. Dissertation, Dept. of Mechanical Engineering and Mechanics, Lehigh Univ., Bethlehem, PA, 1995.

[13]Rockwell, D., Towfighi, J., Magness, C., Akin, O., Corcoran, T., Robinson, O., and Gu, W., "Instantaneous Structure of Unsteady Separated Flows via Particle Image Velocimetry," Fluid Mechanics Labs., Dept. of Mechanical Engineering and Mechanics, Lehigh Univ., Rept. PI-1, Bethlehem, PA, Feb. 1992.

[14]Rockwell, D., Magness, C., Towfighi, J., Akin, O., and Corcoran, T., "High-Image-Density Particle Image Velocimetry Using Laser Scanning Techniques," *Experiments in Fluids*, Vol. 14, No. 3, 1993, pp. 181–192.

[15]Rockwell, D., and Lin, J.-C., "Quantitative Interpretation of Complex, Unsteady Flows via High Image-Density Particle Image Velocimetry," *Optical Diagnostics in Fluid and Thermal Flow*, Proceedings of SPIE, The International Society for Optical Engineering, Vol. 2005, Bellingham, WA, 1993, pp. 490–503.

Correlation of Shock Angles Caused by Flat Delta Wings

S. Koide*
Japan Defense Agency, Tokyo 190, Japan

Introduction

FOR the glancing shock-wave/turbulent-boundary-layer interactions, the inviscid shock wave has an important role for specifying the interaction behavior regardless of the shape of the shock generator. Hence, the trace of the shock wave on the wall provides an important reference position (the imaginary position that would exist if no boundary layer were presented on the wall) for understanding the interaction. The author recently proposed a correlation law for the shock angles caused by a series of rhombic delta wings (RDWs).[1] Using the correlation law, the shock angle on the plane of symmetry of the wing, β, can be predicted easily for a wide range of wing geometries (specified by half-apex angle α and sweep angle λ) and flow Mach numbers M (see Fig. 1a). This angle specifies the trace of shock wave on the wall when a sharp fin, whose cross section is a triangle (the half-cut model of the RDW; see Fig. 1a), is placed on a wall (equivalent to the position of the plane of symmetry for the wing). In this Note, the correlation law is expanded for the delta wings (FDWs). Using the expanded law, the trace of the shock generated by a swept sharp fin can be specified on the wall for various α (angle of attack), λ, and M (see Fig. 1b). The difference of the shock angles caused by the two disparate wings, the RDW and the FDW, is also discussed.

Correlation of the Shock Angles

Unlike the case of the RDWs,[1] several data are available for the FDW shock angles. They have been obtained experimentally by Deng et al.[2] for $6 \leqq \alpha \leqq 20$ deg and $\lambda = 15$ and 50 deg at $M = 2.04$, Fomison and Stollery[3] for $6.5 \leqq \alpha \leqq 35$ deg and $30 \leqq \lambda \leqq 75$ deg at $M = 2.40$, Settles and Lu[4] for $5 \leqq \alpha \leqq 15$ deg and $10 \leqq \lambda \leqq 65$ deg at $M = 2.95$, and computationally by Klunker et al.[5] for $\alpha = 15$ deg and $\lambda = 50$ deg at $M = 4.0$. Based on these data, a correlation of β with M, α, and λ has been considered.

To construct the correlation law for the RDWs, the angle between the plane of symmetry and the face of the delta wing,

$$\xi = \tan^{-1}[1/(\sin\alpha \cdot \tan\lambda)] \tag{1}$$

(see Fig. 1a), was employed. The value expressed by Eq. (1) corresponds to the angle ξ shown in Fig. 1b for the case of the FDWs. By introducing ξ, it is convenient that the two variables α and λ are represented by the single parameter. In the same way for the RDWs, ξ tends to depart from 90 deg when α and λ increase. Similarly β will decrease from its value at $\lambda = 0$ deg (i.e., the oblique shock angle for an unswept sharp fin of half-wedge angle α, expressed by β_{os}) as ξ drops below 90 deg. Hence, it was believed that the angle ξ could be suitable also for correlating the shock angles of the FDWs. As a matter of fact, the same parameter used for the RDWs,

$$(\beta/\beta_{os}) \cdot 2\xi/(\pi M^a) \tag{2}$$

Received Aug. 16, 1995; revision received Nov. 22, 1995; accepted for publication Nov. 30, 1995.

*Senior Research Engineer, 2–5th Laboratory, 3rd Research Center, 1-2-10 Sakae, Tachikawa. Member AIAA.

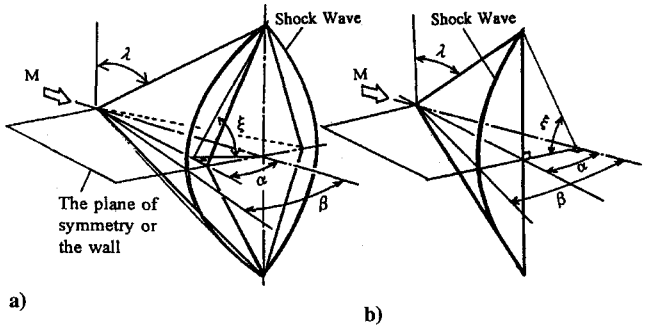

Fig. 1 Schematic view of a) RDW and b) FDW.

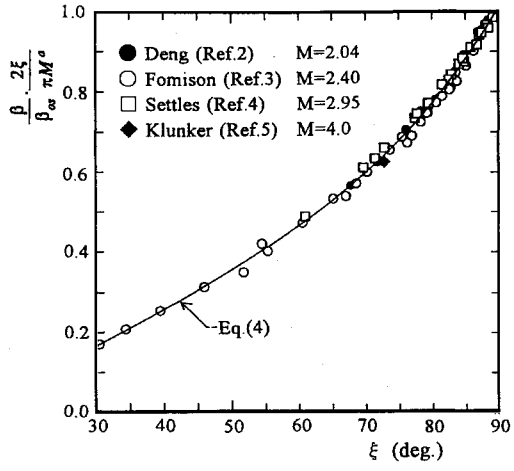

Fig. 2 Correlation of the shock angles.

has been finally proven to correlate the FDW shock angles properly. In the parameter, ξ is expressed in radians and the power a has been selected as $(\pi/2 - \xi)/3$. As shown in Fig. 2, the correlation using the parameter (2) is excellent. The value of β is then determined directly from

$$\beta = \pi\beta_{os} F(\xi) M^a/(2\xi) \tag{3}$$

where $F(\xi)$ has been obtained by the least-squares method as

$$F(\xi) = -0.0202\xi + 1.0204\xi^2 - 0.8885\xi^3 + 0.3234\xi^4 \tag{4}$$

A fourth-order equation was necessary to correlate the data over a wide range of ξ. Each coefficient of the polynomial was different from the value for the RDWs.[1] The difference between the two cases will be discussed in the next section.

Based on the data presented in Fig. 2, the angle predicted by Eq. (3) is quite accurate (within 1 deg of the corresponding experimental value) for the range $0 \leqq \alpha \leqq 21$ deg at all λ and M examined. In terms of Eq. (3), β can be easily specified for various M, α, and λ. It is important to note that this procedure is not applicable for the range where α is above the theoretical attachment limit for the two-dimensional oblique shock at a certain M because β_{os} is not obtainable for Eq. (3) under such a condition.

Why can the simple relation Eq. (3) properly predict the shock angles caused by two disparate shock generators, the RDW and the FDW? During the development of the parameter (2), it has been considered that if β is expressed in the form of a deviation from the well-established theoretical value β_{os}, β can be maintained within a reasonable range even though the values of M, α, and λ change widely. At the same time, β_{os} is a function of M and α, and hence the effects of both values can be included in the single variable β_{os}. Furthermore, β/β_{os} (i.e., the deviation of β from β_{os}) depends on ξ regardless of the combination of α and λ. In both wings, infinite combinations of α and λ are possible for a given ξ. If the wings have different α and λ at a certain M, it is natural that the shock has

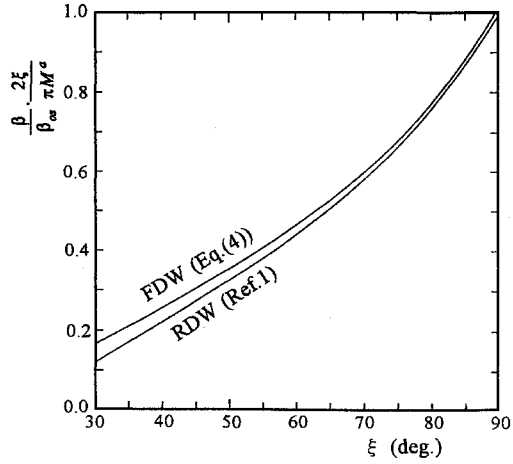

Fig. 3 Comparison of the correlation curves for the RDWs and the FDWs.

a different angle β even though ξ is fixed. But the value of β/β_{os} seems similar as long as ξ and M are the same.

Under these considerations, a simple correlation between β/β_{os} and ξ was first examined but did not sufficiently collapse the data obtained at different M. To improve the correlation, the role of M was further considered. The previous investigation[1] found that β drops less from β_{os} as M increases. As a result, β/β_{os} increased with M for a fixed ξ. This tendency was considered in parameter (2) using the variable M. In addition to the effect of M, it is understood from the relationship linking β, β_{os}, and ξ that β has to approach β_{os} when ξ approaches 90 deg ($\pi/2$ in radians). To satisfy this condition, expressions of $\pi/2 - \xi$ (in the power a) and $2\xi/\pi$ were employed in parameter (2). (Note that the number 3 of the power a was chosen purely for improving the correlation.) Each coefficient of Eq. (4) was also adjusted for Eq. (4) to have a value of 1.0 for the ordinate of Fig. 2 when ξ is 90 deg. Hence Eq. (3) provides β of almost β_{os} when ξ is 90 deg. Consequently, the simple relation Eq. (3) can handle main features of the shock angle properly using a very limited number of variables and can predict the angles even though the geometry of the shock generator is disparate.

Comparison with the Case of the RDW

Figure 3 compares the correlation curves for the cases of the RDWs[1] and the FDWs. At $\xi = 90$ deg, both curves should coincide and have a value of 1.0 for the ordinate of Fig. 3. But a slight error was inevitable because of the approximations using the least-squares method.

From Fig. 3, it is clear that the FDW always has a larger β when both the wings have the same values of α and λ (i.e., the same ξ) at a certain M. It is also noticed that the difference between the two angles for the same α and λ tends to increase when ξ decreases. As Fig. 1 shows, there is a geometrical difference between the two wings. The FDW is perpendicular to the plane of symmetry, whereas the RDW has a certain angle $\xi \leqq 90$ deg. As long as ξ is close to 90 deg, the difference between the two cases is negligible. (Using the two curves in Fig. 3, the difference has been proved to be within 1 deg for the range $\xi \geqq 80$ deg.) But when ξ departs considerably from 90 deg, the FDW shock angle is unlikely to match the value of the RDW.

Conclusions

The correlation law developed for the shock angles caused by RDWs has been expanded for FDWs. The same correlation parameter used for the RDWs, which comprise Mach number, the theoretical two-dimensional oblique shock angle, and an angle representing the wing geometry, has been applicable also for the FDW. Correlation curves for both wings were slightly different. The difference shows that the shock angles by both geometries tend to diverge from each other when the wing sweep angle and apex angle (or angle of attack) increase.

References

[1]Koide, S., Griesel, C. J. W., and Stollery, J. L., "Correlation of Shock Angles Caused by Rhombic Delta Wings," *AIAA Journal* (to be published).

[2]Deng, X., Liao, L., and Zhang, H., "Improvement of Conical Similarity Rules in Swept Shock Wave/Boundary Layer Interaction," AIAA Paper 93-2941, July 1993.

[3]Fomison, N. R., and Stollery, J. L., "The Effects of Sweep and Bluntness on a Glancing Shock Wave Turbulent Boundary Layer Interaction," AGARD CP 428, April 1987.

[4]Settles, G. S., and Lu, F. K., "Conical Similarity of Shock/Boundary-Layer Interactions Generated by Swept and Unswept Fins," *AIAA Journal*, Vol. 23, No. 7, 1985, pp. 1021–1027.

[5]Klunker, E. B., South, J. C., Jr., and Davis, R. M., "Calculation of Nonlinear Conical Flows by the Method of Lines," NASA TR R-374, Oct. 1971.

Counter-Rotating Structures over a Delta Wing

J. P. Hubner* and N. M. Komerath†
Georgia Institute of Technology, Atlanta, Georgia 30332-0150

Nomenclature

b	= wing span
b'	= local wing span
c	= root chord
$G()$	= nondimensionalized autospectral intensity function
L	= characteristic length
n	= Strouhal-scaled frequency, fL/U_∞
Re	= Reynolds number
t	= time
U_∞	= freestream speed
u, v, w	= streamwise, lateral, and vertical velocity, body coordinate system
x, y, z	= body coordinate system, origin fixed to model apex
α	= angle of attack
ϕ	= phase of trigger cycle

Superscripts

-	= time-averaged component of u, v, and w
^	= fundamental periodic component of u, v, and w
'	= random fluctuating component of u, v, and w

Introduction

THIS Note describes the experimental finding of counter-rotating structures, with axes oriented approximately spanwise, located between the surface and the vortex core on a 60-deg delta wing at high incidence. The finding is explained using laser sheet flow visualization and spectral analysis of hot-film data on and above the surface. It is confirmed by quantitative analysis of velocity data, synchronized in phase to the signal from a hot film. The finding is related to previous work on the origin and effects of such fluctuations, and its implications explored. A mechanism based on centrifugal instability is proposed.

Previous work at this and other laboratories[1–5] has shown that the vortex flowfield over a swept wing at 25–35-deg angle of attack develops organized velocity fluctuations under steady freestream conditions. The fluctuations are concentrated within a narrow frequency band but can only be described as quasiperiodic, with the phase not repeating exactly from cycle to cycle. These have been observed on isolated delta wings as well as on wing bodies and full models of fighter configurations. Reference 2 showed that the fluctuations maintain a constant value of reduced frequency (or Strouhal number) at a given angle of attack, over a large range of Reynolds numbers. Data at 20-deg angle of attack near the vertical tail of an F-15 model, extrapolated from $\frac{1}{32}$ and $\frac{1}{7}$ scale model tests using this constant Strouhal number, were shown to match the measured fin vibration frequency on a full-scale F-15. Flowfield studies on moderately swept (<60 deg) wings at angles of attack above 25 deg show that vortex breakdown occurs essentially at the apex. Reference 5 showed that the fluctuations originate close to the wing surface on a 60-deg cropped delta wing at or upstream of the 30% root chord station. They then amplify and focus into a narrow frequency band. The peak frequency decreases as the measurement location is moved downstream. In a crossflow plane at the wing trailing edge, the frequency content is uniform except in the postburst core region, where other phenomena appear to dominate. This Note focuses on the phenomena occurring near the surface. Redionitis et al.[6] attributed the fluctuations to vortex shedding; however, the velocity field over a 60-deg wing at $\alpha < 30$ deg is steady in the mean, and vortex shedding is not a plausible explanation. Gursul[7] proposed a helical mode oscillation in the postburst flowfield characteristic of moderately swept wings. The correlation with experimental evidence for sweep angles >60 deg was encouraging, but the correlation for sweep ≤60 deg was ambiguous. Although the geometry of the flow and the two-point surface pressure correlations of Gursul[7] do allow a helical mode description, this does not complete the physical explanation for the origin, amplification, and focusing of the phenomenon. Here we report on a detailed investigation using multiple planar, surface, and single-point measurement techniques. Spectral content of the fluctuations is measured using both hot films and laser velocimetry (LV). The velocity components are resolved using LV, thereby avoiding the ambiguity inherent in hot-film measurements.

Figure 1 shows the focusing and amplifying of the fluctuation energy for the 59.3-deg delta wing model.[4] The flow unsteadiness is visualized near the surface and under the core using laser sheets illuminated by smoke introduced through various surface ports, aligned parallel and perpendicular to the surface. Surface hot-film sensors and sensors in the flow above the wing are used to generate the spectra of the velocity fluctuations and to determine the frequency

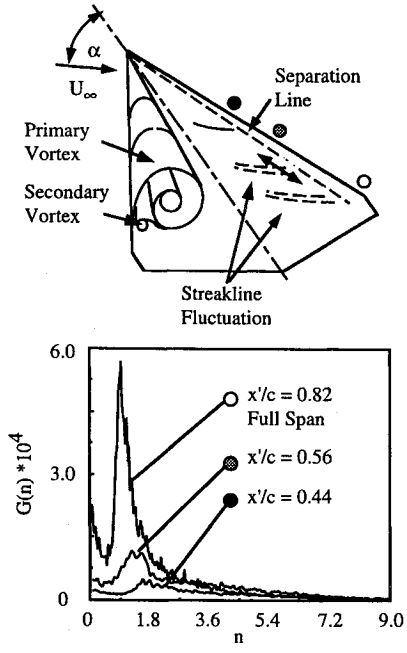

Fig. 1 Autospectra of velocity fluctuations along the leading edge of a 59.3-deg delta wing, measured using a single hot-film sensor oriented spanwise.

Received July 6, 1995; revision received Jan. 9, 1996; accepted for publication Feb. 9, 1996.

*Graduate Research Assistant, School of Aerospace Engineering. Student Member AIAA.

†Professor, School of Aerospace Engineering. Associate Fellow AIAA.